



Interference Power Characterization in Directional Networks and Full-Duplex Systems

Ayman T. Abusabah, Rodolfo Oliveira, Luis Irio

► To cite this version:

Ayman T. Abusabah, Rodolfo Oliveira, Luis Irio. Interference Power Characterization in Directional Networks and Full-Duplex Systems. 12th Doctoral Conference on Computing, Electrical and Industrial Systems (DoCEIS), Jul 2021, Costa de Caparica, Portugal. pp.218-225, 10.1007/978-3-030-78288-7_21 . hal-03685919

HAL Id: hal-03685919

<https://inria.hal.science/hal-03685919>

Submitted on 2 Jun 2022

HAL is a multi-disciplinary open access archive for the deposit and dissemination of scientific research documents, whether they are published or not. The documents may come from teaching and research institutions in France or abroad, or from public or private research centers.

L'archive ouverte pluridisciplinaire **HAL**, est destinée au dépôt et à la diffusion de documents scientifiques de niveau recherche, publiés ou non, émanant des établissements d'enseignement et de recherche français ou étrangers, des laboratoires publics ou privés.



Distributed under a Creative Commons Attribution 4.0 International License

Interference Power Characterization in Directional Networks and Full-Duplex Systems

Ayman T. Abusabah^{1,2}, Rodolfo Oliveira^{1,2}, and Luis Irio²

¹ Departamento de Engenharia Electrónica e de Computadores, Faculdade de Ciências e Tecnologia, Universidade Nova de Lisboa, 2825-149 Caparica, Portugal

² Instituto de Telecomunicações, Portugal

Abstract. This paper characterizes the aggregate interference power considering both directional millimeter-wave (mmWave) and In-Band Full-Duplex (IBFDX) communications. The considered scenario admits random locations of the interferers. The analysis considers a general distance-based path loss with a sectorized antenna model. The interference caused to a single node also takes into account the residual self-interference due to IBFDX operation. The main contribution of the paper is the characterization of the interference caused by both transmitting nodes and full-duplex operation for different parameters and scenarios.

Keywords: In-Band Full-Duplex Wireless Communications, Directional Beamforming, Millimeter-Wave, Interference Characterization, Performance Analysis.

1 Introduction

In In-Band Full-Duplex (IBFDX) wireless communications, the a transceiver can simultaneously transmit and receive over the same frequency band. Compared with half-duplex communication systems, e.g., time division duplexing (TTD) and frequency division duplexing (FDD), the full-duplex systems can potentially double the capacity of the communication link, by reducing the residual self-interference (SI) through passive and active methods [1, 2]. On the other hand, directional communication is a promising technology that has an advantage in overcoming the high isotropic path loss at millimeter-wave (mmWave) bands, [3]. Rigorously speaking, directional communication networks will change the conventional concepts about the interference, because the nodes align their beams according to specific directions.

The characterization of interference in wireless networks has been a topic of extensive research in the last years [4]. The aggregate interference is usually modeled through advanced stochastic geometry techniques [5] that have into account the spatial position of each interferer and its radio channel to determine the amount of interference caused to a specific node [4]. In [6], the authors have adopted the concepts of aligned gain and misaligned gain to derive a coverage model for the signal-to-interference-plus-noise ratio (SINR). The spatial interference caused by multiple simultaneous and uncoordinated transmissions occurring in the mmWave band was studied in [7] to characterize the collision probability as a function of the density of the transmitting nodes and antenna patterns. The authors in [8] have also considered the effect of non-

binary object blockage in the aggregate interference, by assuming that a single obstacle can cause a partial blockage. The modeling of interference in cellular MIMO beamforming mmWave communications was also tackled in [9], by considering two models (inverse Weibull and inverse Gaussian) and a mixture of them. On the other hand, the difficulty in the mathematical modeling process has limited the amount of the study for the statistical characterization of residual SI. The authors in [10] have computed the strength of the residual SI and the amount of cancellation. In particular, the authors assumed a narrow-band model for the characterization of the residual SI power, i.e., it is assumed that the coherence time of the channel is more than the time of the signal. The distribution of the residual SI power was compared with other known distributions in [11]. Closed-form approximations were presented in [12] and [13]. The work in [14] estimates the channel with a single tap delay. While the aforementioned works deal with each type of interference individually, this work considers the characterization of the interference in directional networks jointly with the residual SI from IBFDX systems.

1.1 Motivation and Research Question

The key to success when designing the IBFDX system is to minimize the residual SI. Mainly, the cancelation of the SI is proportional to the accuracy of the estimated channels. Moreover, directional beamforming plays a major role in boosting the communication quality. In such systems, multiple nodes may act as interference sources toward a specific node. Therefore, it is crucial to study the joint interference caused by not only IBFDX systems, but also by directional beamforming. The study aims to answer the following research questions:

- Question 1: What is the best distribution to model the interference power when jointly considering IBFDX and directional communication?
- Question 2: How can the estimation errors effect on the interference power?
- Question 3: What is the influence of gain pattern parameters (main lobe, sidelobes, and beamwidth) on the interference power?

2 Relationship to Applied Artificial Intelligence Systems

Nowadays artificial intelligence (AI) systems play an important role in several sectors, leveraging the added value of a multitude of services through more customized practices that allow a better fit between the service demand and its operational features. Big efforts are usually required to process a large amount of offline data in AI systems, while online applications supported by AI, such as autonomous driving, require very low latency. The low latency requirement includes not only efficient AI algorithms, but also low latency and high throughput communication links. This work is mainly centered on improving the throughput of existing wireless communication systems, which are and will be even more important to deploy a plethora of AI systems capable of addressing mobile and low latency services.

3 System Model

In the system model we consider that the transmitters (aka nodes) are located in the spatial region of interest according to a Poisson Point Process (PPP) Π with density λ over a ring with an inner radius, R_I , and an outer radius, R_O , i.e., $R_I \leq r \leq R_O$. For the particular case of $R_I = 0$ a circular region is considered. Without loss of generality, we condition on a node at the origin, which according to Slivnyak's theory in stochastic geometry [15], yields to a homogeneous PPP with the corresponding density λ . The reference node is supposed to perform IBFDX to communicate with a corresponding node. At a given time slot, we assume that one or more nodes, except the one connected with the reference node, cause interference. The goal is mainly to characterize the power of the interference caused by multiple transmitting nodes and the residual SI power caused by IBFDX operation.

We adopt an active analog canceler full-duplex model [13] that cancels the SI at the angular carrier frequency $\omega_c = 2\pi f_c$. The model considers the residual interference after the SI signal has been canceled by a generic post-mixer active analog canceler. Analogue cancellation schemes can achieve a substantial amount of cancellation [10] (up to 40-50 dB), achieving higher cancellation than the digital one. This can be due to the cancellation of the transmitter impairments. Moreover, if analog cancellation and digital cancellation are sequentially combined, the performance of the digital cancellation depends on the analog cancellation performance, as reported in [16]. Consequently, it is recommended to use analog cancellation techniques before the digital cancellation. The proposed model considers the residual SI signal in an analog post-mixer canceler after the SI signal is upconverted.

The up-converted SI signal, $x(t)$, is transmitted over the full-duplex channel with gain and delay denoted by h and τ , respectively. The estimated channel parameters, delay and gain, $\hat{\tau}$ and \hat{h} , respectively, are injected in the cancellation loop to obtain the residual SI signal, $y_{res}(t)$, as depicted in Fig. 1.

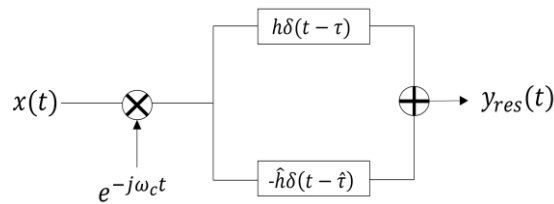


Fig. 1. Block diagram of IBFDX system.

Based on Fig. 1, $y_{res}(t)$ represents the residual SI signal which can be expressed as follows

$$y_{res}(t) = hx(t - \tau)e^{j\omega_c(t-\tau)} - \hat{h}x(t - \hat{\tau})e^{j\omega_c(t-\hat{\tau})}, \quad (1)$$

where h is the channel gain and \hat{h} is the estimated gain given by $\hat{h} = \epsilon h$, where $(1 - \epsilon)$ is the estimation error of the gain, $\epsilon \geq 0$. The estimation error of the phase is given by $\phi = \omega_c(\tau - \hat{\tau})$. We highlight that The estimated channel parameters \hat{h} and $\hat{\tau}$ can be done using different approaches that are already available in the literature [17].

Considering that $x(t - \tau) = x(t - \hat{\tau})$, then (1) can be written as follows

$$y_{res}(t) = x(t)hc, \quad (2)$$

where $c = (e^{j\omega_c(t-\tau)} - \epsilon e^{j\omega_c(t-\hat{\tau})})$ is a constant. Assuming that $x(t)$ and h are independent random variables (RVs), then, the residual SI power can be represented as

$$P_{y_{res}} = (X^2)(H^2)C, \quad (3)$$

where $C = (1 + \epsilon^2 - 2\epsilon\cos(\phi))$ is again a constant. Based on (3), the residual SI power is proportional to the power of the transmitted signal, the power of the SI channel, and estimation errors.

Considering a large-scale, distance-based path loss and small-scale fading for modeling the wireless channel between any communicating pairs. Therefore, the received power caused by an i -th node and seen at the reference node is given by

$$P_i = P_t \Psi_i G_{i,j} G_{j,i} (r_i)^{-\alpha}, \quad (4)$$

where P_t is the same transmitted power across all nodes. We also consider both Rayleigh and Rician small-scale fading channels in which Ψ_i is drawn from a Gamma distribution as shown later. $G_{i,l}$ and $G_{l,i}$ represent the gain of an i -th transmitting node and the gain of the reference node, respectively. $\alpha > 2$ is the large-scale path loss coefficient, and r_i is the distance between an i -th node and the reference node.

The Rayleigh channel can describe the stochastic fading when there is no line-of-sight (LoS) signal. When the channel is a Rayleigh distributed, Ψ_i can be drawn from an exponential distribution with mean $1/\mu$, therefore, it can be expressed by a Gamma distribution with the shape parameter, $k = 1$, and the scale parameter, $\theta = \frac{1}{\mu}$, as follows

$$\Psi_i \sim \text{Exp}(\mu) \sim \text{Gamma}(k, \theta). \quad (5)$$

On the other hand, the Rician fading channel can be characterized through K and Ω where K is the ratio between the LoS power and the non-LoS power, and Ω represents the total power from LoS and non-LoS. Then, the received signal amplitude is Rician distributed with parameters $\nu^2 = \frac{K\Omega}{1+K}$ and $\sigma^2 = \frac{\Omega}{2(1+K)}$. $K_{dB} = 10\log_{10}(K)$ is the decibels representation of K . By definition, if $X \sim \text{Rice}(\nu, \sigma)$, then $(\frac{X}{\sigma})^2$ follows a non-central Chi-squared distribution with non-centrality parameter $(\frac{\nu}{\sigma})^2$. Consequently, moment matching can then be used to obtain a simplified Gamma approximation for

Ψ_i as $\Psi_i \sim \text{Exp}(\mu) \sim \text{Gamma}(k, \theta)$, where the shape parameter, k , and scale parameter, θ , are given by [18]

$$k = \frac{(v^2 + 2\sigma^2)^2}{4\sigma^2(v^2 + \sigma^2)}, \theta = \frac{4\sigma^2(v^2 + \sigma^2)}{(v^2 + 2\sigma^2)^2}. \quad (6)$$

Regarding the beamforming model, we assume that all nodes are capable of performing directional beamforming. We adopt an antenna model to represent the gain patterns G_T and G_R at the transmitting and receiving node, respectively, as follows

$$G_{T,R}(\theta) = \begin{cases} G_{T,R}^{max}, & |\theta| \leq \omega/2 \\ G_{T,R}^{min}, & |\theta| \geq \omega/2 \end{cases} \quad (7)$$

where G^{max} and G^{min} are the gains of main and sidelobes, respectively, defined by beamwidth $\omega \in (0, 2\pi)$ and the bore-sight angle direction $\theta \in (-\pi, \pi)$. We assume that all nodes are located on the same plane, i.e., no variation in beam pattern over the elevation angle. While the sectorized antenna modeling is quite simple, some useful applications with some simplifying assumptions can be obtained and utilized as claimed in [5] and adopted in [13] for establishing innovative MAC policies.

Based on (4), the aggregate interference power caused to the reference node is formulated as

$$I_o = \sum_{i=1}^N P_i, i \in \Pi, \quad (8)$$

where N is a RV characterized by a homogeneous PPP that represents the number of active transmitters over the region represented by the area $A = \pi(R_o^2 - R_f^2)$. Therefore, the probability of n nodes being inside a region A is given by

$$P[N = n] = \frac{(\lambda|A|)^n}{n!} e^{-\lambda|A|}. \quad (9)$$

Finally, the aggregate interference power at the reference node is the residual SI power given by (3) and the interference power given by (9), which can be written as

$$P_{tot} = P_{y_{res}} + I_o. \quad (10)$$

4 Performance Analysis

The validation has been performed using the Monte Carlo simulation results where 10^6 iterations were run. The carrier frequency is set to 60 GHz. The power of the residual SI in (3) and the aggregate interference power in (8) are generated from empirical data. The samples of the SI signal are generated from Normal distribution, i.e., $X \sim \mathcal{N}(0, \sigma_x^2)$ with $\sigma_x^2 = \frac{1}{2}$. The SI channel is assumed to be Rician distributed, i.e., $H \sim \text{Rice}(v, \sigma)$. Ψ_i are generated from a Gamma distribution, where k and θ are

identified for a Rayleigh channel and for a Rician channel. The network and channel parameters are listed in Table 1, unless otherwise specified.

Table 1. Network and channel parameters

f_c	60 GHz	P_t	1 mW	σ_x^2	0.5	Ω	1 mW
ϵ	0.9	K_{dB} for SI channel	10	σ_h^2	0.5	α	4
ϕ	10°	K_{dB} for directional channel	0	R_I, R_O	1 m, 5 m	G^{max}	1
μ	2	ω	$\{45^\circ, 60^\circ\}$	λ	50 node / m ²	G^{min}	$\{0.05, 0.1\}$

For sake of defining the best distribution in representing the aggregate interference power, different known distributions were generated using empirical data . Fig. 2 plots the PDF of the distributions exhibiting the best accuracy (Exponential, Weibull, Nakagami, Gamma, Rayleigh, Generalized Extreme Value (GEV), and Lognormal) against the PDF of the empirical data considering a Rician Fading channel for directional communication. As can be seen, GEV distribution exhibits the best accuracy in representing the aggregate interference power. The CDFs of the aggregate interference power are depicted in Fig. 2 for fast fading (Rician and Rayleigh) channels. Different gain levels of the beam sidelobes and different beamwidths are considered. The results reflect the incremental

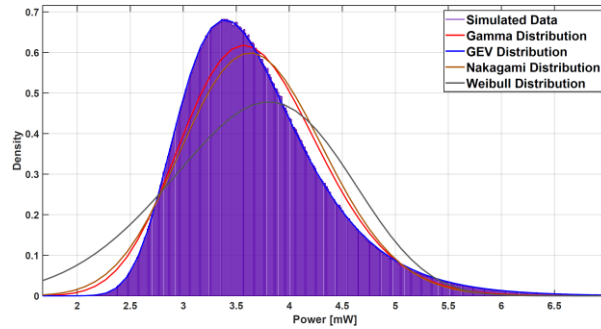


Fig. 2. The PDF of the aggregate interference power with PDFs of other known distributions considering a Rician channel for directional communication: $K_{dB} = 0$, $\omega = 45^\circ$, and $G^{min} = 0.1$.

effect on the interference power due to the increase in the sidelobes gain ($G^{min} = 0.05, 0.1$ were adopted in the comparison). On the other hand, the results show that the interference power decreases when adopting small ω values (narrower beams), due to the concentration of higher power in specific and smaller spatial regions ($\omega = 45^\circ, 60^\circ$ were adopted in the comparison). We conclude that although the proposed modeling methodology is quite simple, the simulated CDFs comply with different network and channel parameters.

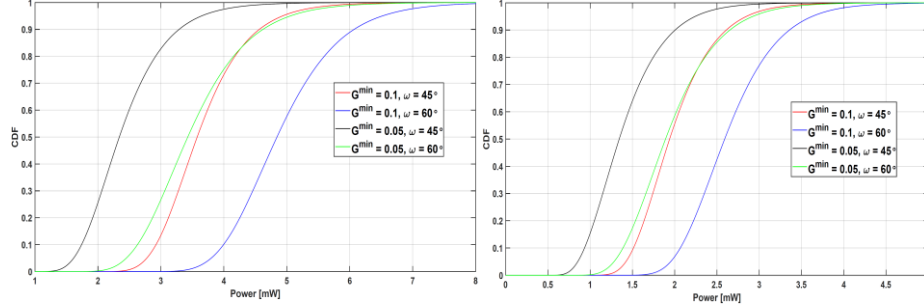


Fig. 3. CDFs of the aggregate interference power P_{tot} considering 1) a Rician fading channel for directional communication with $K_{dB} = 0$ at the left side 2) a Rayleigh fading channel for directional communication: $\mu=2$ at the right side.

5 Conclusions

In this paper, we have studied the distribution of the aggregate interference power due to: 1) the residual SI power in IBFDX, 2) the interference caused to a single node in directional beamforming networks. The work takes the initial step for investigating theoretical approximations of the aggregate interference power. Based on an extensive comparison with known distributions, it is shown that the GEV distribution exhibits the best accuracy in representing the aggregate interference power. The aggregate interference power distribution shown in this work can be adopted in providing technical criteria for mitigating the level of the interference in practical directional communication when considering IBFDX systems. For example, the optimal antenna parameters can be computed according to a given interference level. In general, the interference characterization can be utilized to define several points related to the performance analysis of both directional communication and IBFDX systems. For instance, the communication systems capacity can be enhanced by deriving the outage probability using the characteristics of the aggregate interference power.

Acknowledgements

This work was supported by the Marie Skłodowska-Curie project number 813391, TeamUp5G.

References

1. K. E. Kolodziej, B. T. Perry and J. S. Herd, "In-Band Full-Duplex Technology: Techniques and Systems Survey," in *IEEE Trans. on Microw. Theory Tech.*, vol. 67, no. 7, pp. 3025-3041, July 2019.

2. G. C. Alexandropoulos and M. Duarte, "Joint design of multi-tap analog cancellation and digital beamforming for reduced complexity full duplex MIMO systems," *IEEE International Conference on Communications (ICC)*, Paris, 2017, pp. 1-7.
3. H. Yang, M. H. A. J. Herben, I. J. A. G. Akkermans and P. F. M. Smulders, "Impact Analysis of Directional Antennas and Multiantenna Beamformers on Radio Transmission," in *IEEE Trans. on Veh. Technol.*, vol. 57, no. 3, pp. 1695-1707, May 2008.
4. Martin Haenggi and Radha Ganti. Interference in large wireless networks. *Foundations and Trends in Networking*, 3:127–248, 01 2009.
5. M. Di Renzo, "Stochastic Geometry Modeling and Analysis of Multi-Tier Millimeter Wave Cellular Networks," in *IEEE Trans. on Wireless Comm.*, vol. 14, no. 9, pp. 5038-5057, Sept. 2015.
6. M. Rebato, J. Park, P. Popovski, E. De Carvalho and M. Zorzi, "Stochastic Geometric Coverage Analysis in mmWave Cellular Networks with Realistic Channel and Antenna Radiation Models," in *IEEE Trans. on Commun.*, vol. 67, no. 5, pp. 3736-3752, May 2019.
7. S. Singh, R. Mudumbai and U. Madhow, "Interference Analysis for Highly Directional 60-GHz Mesh Networks: The Case for Rethinking Medium Access Control," in *IEEE/ACM Trans. on Netw.*, vol. 19, no. 5, pp. 1513-1527, Oct. 2011.
8. S. Niknam, B. Natarajan and R. Barazideh, "Interference Analysis for Finite-Area 5G mmWave Networks Considering Blockage Effect," in *IEEE Access*, vol. 6, pp. 23470-23479, 2018.
9. H. Elkotby and M. Vu, "Interference Modeling for Cellular Networks Under Beamforming Transmission," in *IEEE Trans. on Wireless Commun.*, vol. 16, no. 8, pp. 5201-5217, Aug. 2017.
10. Sahai, G. Patel, C. Dick, and A. Sabharwal, "On the impact of phase noise on active cancellation in wireless full-duplex," *IEEE Trans. Veh. Technol.*, vol. 62, no. 9, pp. 4494–4510, Nov 2013.
11. A. T. Abusabah, L. Irio and R. Oliveira, "In-Band Full-duplex Residual Self-interference Approximation in Multi-tap Delay Fading Channels," 2020 *International Wireless Communications and Mobile Computing (IWCMC)*, Limassol, Cyprus, 2020, pp. 635-640.
12. A. T. Abusabah, L. Irio, R. Oliveira and D. B. da Costa, "Approximate Distributions of the Residual Self-Interference Power in Multi-tap Full-Duplex Systems," in *IEEE Wireless Commun. Lett.*, doi: 10.1109/LWC.2020.3042754.
13. L. Irio and R. Oliveira, "Distribution of the Residual Self-Interference Power in In-Band Full-Duplex Wireless Systems," in *IEEE Access*, vol. 7, pp. 57516-57526, 2019.
14. A. Quazi, "An overview on the time delay estimate in active and passive systems for target localization," in *IEEE Trans. Acoust., Speech, Signal Process.*, vol. 29, no. 3, pp. 527-533, June 1981.
15. Baccelli and B. Blaszczyzyn. *Stochastic Geometry and Wireless Networks*. Delft, The Netherlands: Now Publishers, Sep.2009.
16. M. Duarte, "Full-duplex wireless: Design, implementation and characterization," Ph.D. dissertation, Rice Univ., Houston, TX, USA, Apr. 2012.
17. Y. Choi and H. Shirani-Mehr, "Simultaneous Transmission and Reception: Algorithm, Design and System Level Performance," in *IEEE Trans. on Wireless Commun.*, vol. 12, no. 12, pp. 5992-6010, December 2013.